

**VALIDATION AND LOCALIZATION OF RESTRICTED GENE
EXPRESSION IN THE DEVELOPING PROSTATE**

by

Sander Barkley Frank

A thesis submitted to the Faculty of the University of Delaware in partial fulfillment of the requirements for the degree of Honors Bachelor of Arts in Biological Sciences with Distinction.

Spring 2009

Copyright 2009 Sander Frank
All Rights Reserved

**VALIDATION AND LOCALIZATION OF RESTRICTED GENE
EXPRESSION IN THE DEVELOPING PROSTATE**

by

Sander Barkley Frank

Approved: _____
Robert A. Sikes, Ph.D.
Professor in charge of thesis on behalf of the Advisory Committee

Approved: _____
Kenneth Van Golen, Ph.D.
Committee member from the Department of Biological Sciences

Approved: _____
Sharon Rozovsky, Ph D.
Committee member from the Board of Senior Thesis Readers

Approved: _____
Alan Fox, Ph.D.
Director, University Honors Program

DEDICATION

This thesis, my most prized undergraduate accomplishment, is dedicated to my mother, Terrie Barkley Frank, whose memory I hold dearly as I begin my career and take part in the fight of ever-advancing human understanding against cancer, a continuing plague against humanity.

ACKNOWLEDGMENTS

I would like to acknowledge those who helped me complete this project. Shegnan Zhang, who helped optimize annealing temperatures for some of the PCR primers. Laretta Ovadaje, who worked before I came to the lab organizing the microarray data into categories. The University of Delaware Office of Laboratory Animal Medicine (OLAM) for help maintaining mice colonies. Dr. Kirk Czymmek of the University of Delaware Bio-imaging Center for his aid in confocal microscopy. I would also especially like to thank Qian “Cynthia” Chen, who helped teach me how to perform most of the experiments utilized in my project, especially the UGS microdissections. She helped me greatly with nearly every aspect of my project and supported me throughout my undergraduate research career. I also want to thank Professor Robert Sikes, who allowed me to work in his lab and offered knowledge and advice for how to organize and troubleshoot this project. And lastly thanks to my family who support me in every aspect of my life. Personal funding was supplied by the University of Delaware Undergraduate Research Program through a Science and Engineering summer fellowship and Milton Stetson memorial summer fellowship. Project funding was supplied through NIH R01 DK63919.

TABLE OF CONTENTS

LIST OF TABLES	vii
LIST OF FIGURES	viii
LIST OF TERMS AND ABBREVIATIONS	ix
ABSTRACT	x
Chapter	
1 INTRODUCTION	1
1.1 Diseases of the Prostate.....	1
1.1.1 Benign Prostatic Hyperplasia (BPH).....	1
1.1.2 Prostate Cancer (PCa).....	2
1.1.3 Economic Strain.....	3
1.2 Prostate Anatomy.....	3
1.2.1 Mouse Model.....	4
1.2.2 Prostate Development: Urogenital Sinus (UGS).....	4
1.2.3 Compartments of the UGS	5
1.3 Importance of Studying Prostate Development	7
1.4 Project Outline	7
2 EXPERIMENTAL METHODS	9
2.1 Animal Recourse and Tissue Collection	9
2.2 mRNA Validation.....	11
2.2.1 RNA Extraction	11
2.2.2 cDNA Synthesis	11
2.2.3 Primer Design.....	12
2.2.4 Quantitative Real-Time PCR (Q-PCR).....	12
2.3 Protein Validation	14

	2.3.1	Immunofluorescence (IF).....	14
	2.3.2	Western Blot (WB)	16
3		RESULTS	17
	3.1	Custom cDNA Microarray (MA).....	17
	3.2	Quantitative PCR (Q-PCR)	23
		3.2.1 Male Female Differences	24
		3.2.2 Cross Check for Primary Compartment Genes	24
	3.3	Immunofluorescence (IF).....	32
	3.4	Western Blot (WB)	37
4		DISCUSSION	38
	4.1	Tissue Recourse	38
	4.2	Microarray (MA).....	39
	4.3	Reasoning Behind Gene Selection For Validation	40
	4.4	Quantitative PCR (Q-PCR)	41
		4.4.1 Male Versus Female Differences.....	42
		4.4.2 Cross Check For Primary Compartment Genes	42
	4.5	Protein Validation	43
	4.6	Summary.....	44
		REFERENCES	446

LIST OF TABLES

2.1	Oligonucleotide primer information.	13
2.2	Table showing antibody information.	15
3.1	Selection of microarray results listed by functional catagories.	18
3.2	Reference table for Log_2 scale => fold change conversion.	25

LIST OF FIGURES

1.1	Diagram illustrating the compartments of the UGS.	6
2.1	Diagram depicting the procedure for microdissection of the UGS.	10
3.1	Primary compartment mRNA localization by Q-PCR.	26
3.2	Epithelial secondary compartment mRNA localization by Q-PCR.	27
3.3	Mesenchymal secondary compartment mRNA localization by Q-PCR	28
3.4	Q-PCR results for secondary compartment genes in Cartesian.	29
3.5	Q-PCR results of male versus female mRNA differences.	30
3.6	Q-PCR results of UGD/UGV primary genes cross checked for UGE/UGM differences.	31
3.7A	IF staining for Tpm2 (UGM predicted) and Cdh1 (UGE predicted).	33
3.7B	IF staining for Myh3 (UGV predicted).	34
3.7C	IF staining for Msc (VM predicted)	35
3.7D	IF staining for Fgfr2 (DE predicted).	36
3.8	Western blot results for Myh3 and Pax2.	37

LIST OF TERMS AND ABBREVIATIONS

Anatomy:

UGS – Urogenital Sinus
UGE – Urogenital Epithelium
UGM – Urogenital Mesenchyme
UGD – Urogenital Dorsal
UGV – Urogenital Ventral
DE – Urogenital Dorsal and Epithelial
DM – Urogenital Dorsal and Mesenchymal
VE – Urogenital Ventral and Epithelial
VM – Urogenital Ventral and Mesenchymal

Techniques:

IF – Immunofluorescence
MA – Microarray
Q-PCR – Quantitative real-time reverse transcription polymerase chain reaction
RT-PCR – Reverse Transcription PCR
WB – Western blot

Other Abbreviations:

BPH – Benign Prostatic Hyperplasia
cDNA – Complementary DNA
DRE – Digital Rectal Exam
DMEM – Dulbecco's Modified Eagle Medium
E16.5 – Embryonic day 16.5
FITC – Fluorescein Isothiocyanate
HRP – Horseradish Peroxidase
IgG – Immunoglobulin
OCT – Optimal Cutting Temperature
PBS – Phosphate Buffered Saline
PCa – Prostate Cancer
PSA – Prostate Specific Antigen
RIPA – Radioimmunoprecipitation Assay
Ta – Annealing Temperature

ABSTRACT

The prostate gland is a significant source of male genitourinary tract morbidity. As developmental processes share several features in common with metastatic cancer, I hypothesize that a better understanding of genes involved in prostate morphogenesis may identify possible targets for therapeutic intervention. The prostate is derived from the urogenital sinus (UGS), which can be separated into four subdomains based on cellular compartment and dorsal-ventral patterning: epithelium/mesenchyme (UGE/UGM) and dorsal/ventral halves (UGD/UGV). Each region develops into specific lobes of the prostate with unique structural and biochemical properties. My research sought to validate differential gene expression associated with each of these UGS subcompartments as determined by a survey of more than 15,000 cDNA fragments in a custom microarray covering a timed course of prostate development. Results identified 530 genes (3.5%) in UGE/UGM, and 35 (0.23%) in UGD/UGV that exhibit spatially restricted expression in UGS subdomains. To validate the microarray results, male UGS were separated either into UGE/UGM or UGD/UGV subcompartments. Total RNA was extracted and used to synthesize cDNA templates for each subdomain. Quantitative real time reverse transcription polymerase chain reaction (Q-PCR) was performed to observe relative mRNA levels and confirm localization for 10/12 primary and 6/10 secondary compartmental genes. Immunofluorescence (IF) was used to localize 5 genes in the predicted subdomains. With this research I have established a map of regional gene expression in the murine UGS and identified candidate genes for further study and analysis.

Chapter 1

INTRODUCTION

1.1 Diseases of the Prostate

The prostate gland is a very complex organ and is highly susceptible to disease, particularly in older men of Western civilizations. The most common disease is benign enlargement of the prostate caused by increased proliferation known as benign prostatic hyperplasia. However, prostate cancer has high incidence rates as well. Furthermore, the prostate is susceptible to infections, though these diseases are less common than the two previously mentioned.

1.1.1 Benign Prostatic Hyperplasia (BPH)

The most common disease associated with the prostate is Benign Prostatic Hyperplasia (BPH), a non-cancerous enlargement of the prostate. The prostate enlarges to some extent in all men as they age, and by age 60 about half of all men will have BPH, while the vast majority of men who live to their seventies and eighties will experience symptoms of BPH.(1) BPH also has a significantly higher incidence rate in African American males when compared to their White counterparts.(2) An enlarged prostate adds pressure to the bladder and urethra. Basic symptoms of BPH include frequent urges and weak urinary flow, while more severe symptoms include bladder stones and sexual dysfunction.(2) The current standard for BPH detection is either an ultrasound or digital rectal exam (DRE), where a doctor can feel for prostate

enlargement or irregularity through the rectal wall. Treatment for mild cases includes hormone therapy and drugs, while more severe cases are usually treated by surgery. The current surgical trend has been to move away from an invasive open prostatectomy to more minimally invasive surgeries or laser treatments with less recovery time and side effects.(3) It is also important to note that BPH, while very common, has not been shown to lead directly to prostate cancer.(1) However, BPH and prostate cancer do share enough similarities in pathogenesis and epidemiology that some researchers suspect a connection, particularly with fast growing BPH.(4)

1.1.2 Prostate Cancer (PCa)

Prostate cancer (PCa) is the most commonly diagnosed non-cutaneous cancer in American men and remains the second leading cause of cancer deaths. One in six men is likely to develop PCa in his lifetime. There were an estimated 186,000 new cases of PCa in 2008 and 28,000 estimated deaths.(5) There is some familial heredity associated with the disease, most notably the HPC1 gene.(6) Men with a close relative, particularly a brother or father who had PCa, are between 1.5 and 3 times more likely to develop the disease than someone with no family history.(7) There also have been a few rare cases where a virus may be responsible for HPC1 mutations.(8) Prostate cancer symptoms are often subtle and resemble those of BPH; screenings are also similar, utilizing DRE and Prostate Specific Antigen (PSA) screening, a general PCa marker.(9) PCa is treatable with early detection when it remains localized in the prostate. Treatments vary but include radiation, prostatectomy, and hormone ablation therapy, all of which have effects ranging from urinary incontinence to impotence.(6) The lethal phenotype of PCa results primarily from metastasis, especially to bone and

the spine, which creates a cytokine imbalance leading to cachexia, hematocytopenia, pain, and poor prognosis.(10)(11)

1.1.3 Economic Strain

The high prevalence of prostatic diseases like BPH and PCa lead to a large economic burden. It is estimated that BPH has a total cost of 3.9 billion dollars a year, which includes direct medical costs for employers and insurance companies as well as indirect costs such as lost labor.(12) Furthermore, BPH costs patients an average of \$1,500 per year.(12) PCa health care costs average around \$26,000 over 3 years, and up to \$48,000 for hormone ablation therapy.(13) The costs associated with PCa are 3rd behind lung and colorectal cancer. Initial Medicare costs for individual PCa treatment were at \$18,000 in 2002, while the overall cost to the United States is estimated at 2.3 billion dollars over five years.(14)(15)

1.2 Prostate Anatomy

The prostate is a small, partially muscular gland located around the urethra and below the male bladder. It is a part of the urogenital system and functions together with the kidneys, bladder, and reproductive system. The human prostate gland is composed of three zones: peripheral, central, and anterior.(16) The prostate is regulated by androgens, particularly testosterone, and is highly innervated.(17)(18) The main function of the prostate is to release prostatic fluid, which aides the release and viability of sperm during ejaculation.(19) Sperm travel from the testes through the vas deferens to the seminal vesicle, which contributes seminal fluid to the prostatic fluid and forms semen.

1.2.1 Mouse Model

Mice have long been used in the science world as a tool for working with human diseases, and the mouse prostate serves as a decent analogue.(20) The mouse prostate is not exactly like a human prostate, but it has analogous lobes: Anterior, Dorsal, Lateral, and Ventral. The dorsal and lateral lobes are most similar to the human peripheral zone, where ~90% of PCa originates.(16)

1.2.2 Prostate Development: Urogenital Sinus (UGS)

Both mice and humans have a urogenital sinus (UGS), which is the prostatic anlagen, or prostate progenitor, in males. While oversimplified, the UGS basically is composed of an endodermally derived epithelial tube (UGE) surrounded by a mesodermally derived outer layer of mesenchymal tissue (UGM). At embryonic day 16.5 (E16.5), the UGE in males begins to evaginate or form epithelial buds that invade the adjacent mesenchyme (UGM) and eventually give rise to the lobes of the adult prostate gland. The bidirectional interaction between UGM and UGE is critical for prostate organogenesis.(21) The UGE is androgen insensitive but can be regulated by androgen through the androgen sensitive UGM.(22)(23) In addition, the dorsal UGS (UGD) develops into the anterior and dorsal prostate while the ventral UGS (UGV) develops into the ventral prostate.(24) The lateral prostate lies midway between the dorsal and ventral prostates and has been grouped predominantly with the dorsal prostate.(25) These lobes each have their own unique properties beyond anatomic location that include the lobular structure, secretory proteins, and their relationship to prostatic diseases.(24)

1.2.3 Compartments of the UGS

My project focused on confirming the spatially restricted pattern of gene expression located in specific subdomains of the UGS. I designated compartments based on two factors: 1) tissue type; epithelium/mesenchyme (UGE/UGM) and 2) physical location; dorsal/ventral (UGD/UGV). With these distinctions, there are four possible primary compartments: UGE, UGM, UGD, or UGV. The first groups of genes were predicted by microarray screening of gene expression to exhibit a difference in *either* UGE/UGM *or* UGD/UGV, but not both. For example, a gene may be ten fold in UGE versus UGM, but have no UGD/UGV difference.

A second group of genes in UGS subdomains exhibited a difference in *both* UGE/UGM *and* UGD/UGV simultaneously. This leads to four new possible restricted expression profiles: dorsal epithelial (DE), ventral epithelial (VE), dorsal mesenchymal (DM), or ventral mesenchymal (VM). For example, a gene may be five fold UGE over UGM, *and* eight fold UGD over UGV, thus making it DE localized.

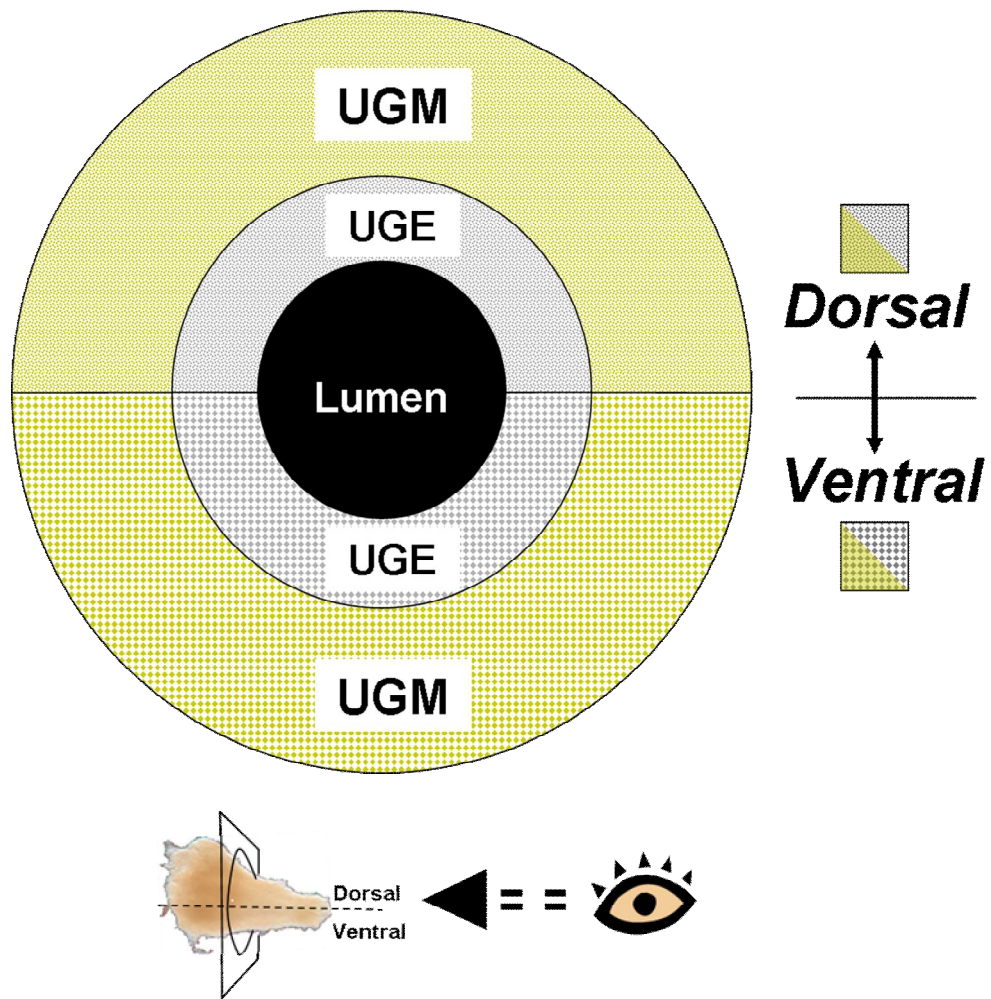


Fig. 1.1 Diagram illustrating the compartments of the UGS. This cross sectional view shows the inner epithelial tube (UGE) surrounded by an outer layer of mesenchyme (UGM), each with a dorsal (UGD) and ventral (UGV) half. Primary compartment genes only show a difference in UGE/UGM or UGD/UGV, while secondary compartment genes are differentially expressed in both the UGE/UGM and UGD/UGV.

1.3 Importance of Studying Prostate Development

The prostate is a very complicated and disease-prone organ, and it is crucial to increase understanding of the developmental process if we are to fully understand this organ. The key to proper organ development is tight regulation of a multitude of different growth factors, transcription factors, and other organizational genes. Since organogenesis involves highly restricted and controlled gene expression for growth, it is very likely that a disruption in these genes would lead to uncontrolled growth and organization (i.e. cancer). In line with this development-disease connection, at least one current theory believes that prostatic hyperplasia is the result of re-activated developmental growth signals.(26) There is also an abundance of evidence linking developmental genes to cancer.(27)(28)(29)(30)

1.4 Project Outline

My research sought to identify genes whose expression profiles were distributed uniquely in the urogenital sinus, thereby providing a diagram of restricted gene expression corresponding to developmental outcome or predetermination of a prostatic lobe prior to the initiation of budding. The UGS was enzymatically and mechanically dissociated into UGE and UGM or bisected manually into dorsal (UGD) and ventral (UGV) aspects. Microarray analysis was performed on these samples using the mouse prostate expression database (MPEDB) custom cDNA array for prostate development. Significant differences in mRNA expression were detected between UGE versus UGM as well as UGD versus UGV. Bioinformatic analysis of these microarray results determined genes most likely to be differentially expressed in VE, VM, DE or DM. Changes in mRNA levels were confirmed and quantified using Quantitative RT-PCR (Q-PCR) with RNA from isolated subcompartments of the UGS. Protein

localization was examined by immunofluorescence or western blot on sections of E16.5 UGS using confocal microscopy. Identifying differentially expressed genes between the subdomains of the UGS will give researchers some targets for critical genes involved in specific lobular morphogenesis and possibly prostatic disease.

Chapter 2

EXPERIMENTAL METHODS

2.1 Animal Recourse and Tissue Collection

Mice were purchased from Jackson Labs (West Grove, PA) and housed under regulated lighting conditions (12 hr light: 12 hr dark). All breeding and tissue harvest was done in the vivarium under IACUC (Institutional Animal Care and Use Committee) approved research protocols of the Office for Laboratory Animal Management at the University of Delaware. Timed matings were carried out by introduction of male mice to females overnight. Detection of a vaginal copulation plug was designated embryonic day 0.5 (E0.5). Pregnant female mice were sacrificed and whole UGS were dissected at E16.5 under a stereo dissection microscope (SMZ800, Nikon instruments inc., Melville, NY). The UGS were then either: 1) digested in a 1:1 solution of DMEM (Dulbecco's Modified Eagle Medium):DispaseII (Invitrogen, Carlsbad, CA) for four hours on ice to loosen the association between epithelial and mesenchymal tissue, whereupon these subdomains were microdissected from each other, 2) bisected into dorsal and ventral halves; or 3) removed while attached to the bladder and embedded in Optimal Cutting Temperature (OCT) medium (Tissue-tek, Sakura Finetek inc., Torrance, CA) and stored at -80°C until sectioning for immunofluorescence. Additional tissues were harvested exactly as described and stored at -80°C for RNA extraction and protein isolation.

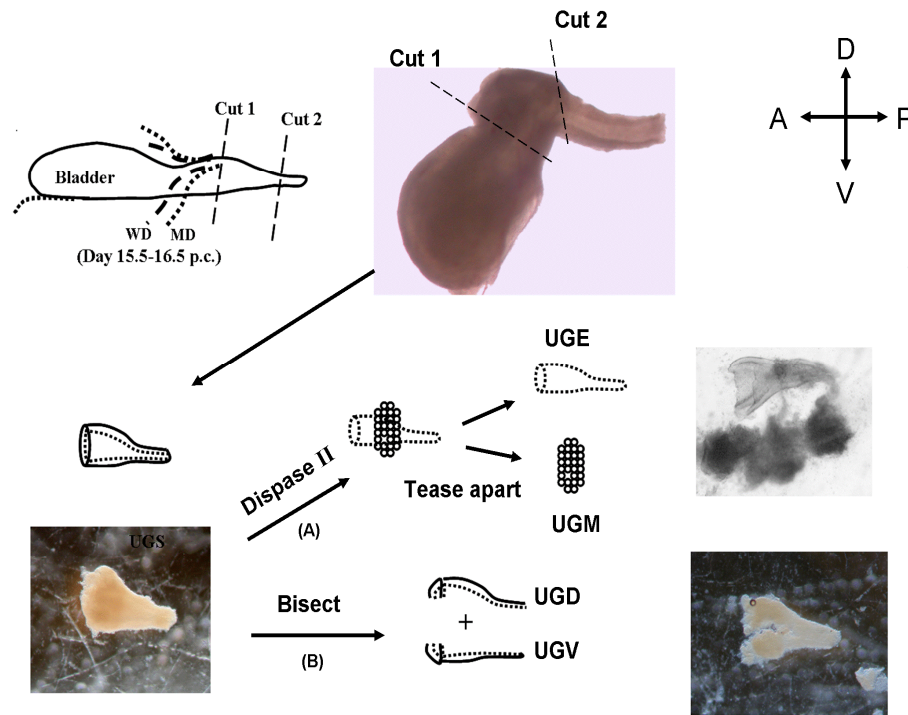


Fig. 2.1 Diagram depicting the procedure for microdissection of the UGS. The UGS is first cut below the bladder and ducts. The UGS is then either digested in DispaseII for at least three hours and then separated into epithelial (UGE) and mesenchymal (UGM) tissues under the microscope (path A), or bisected manually under a microscope into dorsal (UGD) and ventral (UGV) halves (path B). Tissue samples were then used for RNA extraction and then cDNA synthesis for template of each compartment. Some UGS were not cut from the bladder and were mounted in OCT freezing medium to be sectioned for Immunofluorescence.

2.2 mRNA Validation

2.2.1 RNA Extraction

RNA was extracted from six to ten pooled UGS compartment samples using the Trizol reagent kit (Invitrogen) according to the manufacturer's protocol. RNA samples were quantified with a SmartSpec 3000 spectrophotometer (BioRad Lab, Hercules, CA). Approximately 1 μ g of extracted RNA was then run on 1.2% agarose gel in 0.5x Tris-Acetate EDTA buffer (TAE: 40mM tris-acetate, 1mM EDTA, PH 8.0) and stained with ethidium bromide to check RNA quality and confirm that absorbance readings resulted in normalized levels.

2.2.2 cDNA Synthesis

cDNA was synthesized from total extracted RNA using the Superscript III First Strand Synthesis System for RT-PCR (Invitrogen) according to the manufacturer's protocol using 5 μ g of total RNA per 20 μ L reaction. The cDNA product was then run on 1.2% agarose gel and stained with ethidium bromide to check for a DNA smear (1kb-2kb) indicating an appropriate cDNA synthesis. The cDNA was then normalized by running 0.5-1 μ g samples as template with RPL19 primers, a ribosomal housekeeping gene confirmed to have no compartmental specific localization and no change in expression throughout development (data not shown). Normalization was achieved by visual inspection of RPL19 amplification in standard RT-PCR and estimating the dilutions necessary to have relatively equivalent stocks of complementary templates (UGE/UGM and UGD/UGV).

2.2.3 Primer Design

Primers were designed for each gene under observation utilizing software by: Operon (<http://www.operon.com/technical/toolkit.aspx>), Primer3 (http://frodo.wi.mit.edu/cgi-bin/primer3/primer3_www.cgi), and VectorNTI (Invitrogen).⁽³¹⁾ Primers were designed to span large introns so that any DNA contamination would appear as large bands upon inspection by agarose gel electrophoresis or would not be amplified under conditions suited for cDNA detection. The primer information, including oligonucleotide sequence, size, and annealing temperature are in Table 2.1. The optimal primer conditions were: length of 21bp, at least 50% GC content, matching primer melting points (TMs) within 3 degrees, and confirmation that no hairpins or primer dimers were likely, as determined using Vector NTI software. Gradient RT-PCR was then used to find optimal annealing temperatures (see Table 2.1) for each set of primers using a Mastercycler Gradient Thermal Cycler (Eppendorf, Westbury, NY).

2.2.4 Quantitative Real-Time PCR (Q-PCR)

Q-PCR was performed in duplicate for each gene with the proper cDNA templates (UGD/UGV or UGE/UGM) from male E16.5 mice at acceptable annealing temperatures as found by gradient PCR. These reactions were repeated with separate female cDNAs from different sets of fetal UGS tissue isolations. The data were normalized to RPL19. Some genes also were run in conventional RT-PCR with equivalent amounts of different templates to check and visualize relative amplification levels on agarose gels (data not shown).

Table 2.1 Oligonucleotide Primer Information. Forward (F) and reverse (R) primers were designed to span large introns. Table shows gene designation, sequence, product size (base pairs), and annealing temperature (Ta).

Gene	Primer Sequence 5'-3'	Size	Ta	Gene	Primer Sequence 5'-3'	Size	Ta
Ly6e (F)	GCGAACCTTCAGCAGATGTC	170	59	Fgfr2 (F)	CGAGAAGATGGAGAAGCGGC	198	66
Ly6e (R)	TGGTCTTTCTCCTGGCATG			Fgfr2 (R)	TCTGACGGGACCACACTTTC		
Plac8 (F)	CCTGTTTGCTCTGTGTGCCA	164	59	Krtdap (F)	AAGTGCCGCTCCTGATTC	135	59
Plac8 (R)	CCATCCCATCTCAGTTGCCA			Krtdap (R)	TATTGGGGAACTGAGGC		
Tnfrsf19 (F)	CGCTGCCATTCTCCTCCTAC	214	59	Tacstd1 (F)	GTTCCGGGCTCCTGCTCG	198	59
Tnfrsf19 (R)	ACCCAGTCTTCCTTGAACC			Tacstd1 (R)	GTCATTTCTGCTTTCATCGCC		
Tnnc2 (F)	GGGAAGAGCGAAGAGGAACT	168	59	Wnt4 (F)	ACTCCTCGTCTTCGCCGTGT	159	66
Tnnc2 (R)	GCCGTCGTTGTTTTATCACC			Wnt4 (R)	ATCACCTCAAGGTTCCGTTTGC		
Myh3 (F)	TGAGTAGCGACACCGAGATGG	228	66	Grm7 (F)	CAGAAGGAGCCATCACCATC	119	59
Myh3 (R)	CGTCCTCTGGCTTAACCACC			Grm7 (R)	TTCCAGTATTCGGCAAACC		
Pax2 (F)	CTTTAAGAGATGTGTCTGAGG	193	59	Ntrk2 (F)	CGTCTGGCTGCTCCTAACCTC	146	66
Pax2 (R)	TCATTCCCCTGTTCTGATTTG			Ntrk2 (R)	CCCTGTGTGTGGCTTGTTTCA		
Adh1 (F)	GTGGGTTCTCAACTGGCTATG	98	59	Ogn (F)	CTTCCAGTTCTCCTCCAA	144	59
Adh1 (R)	AGACAGACCGACACCTCCG			Ogn (R)	AGGCACAGATTCCAGGTC		
Pdzk1ip1 (F)	CCAGGAGTCAAAAACACCAG	177	66	Phox2b (F)	GCTGAGACGCACTACCCTGAC	121	66
Pdzk1ip1 (R)	CCAAGAACACAGCGACAGC			Phox2b (R)	GCTCCTGCTTGCGAAACTTAG		
lox (F)	CCGCAAAGAGTGAAGAACCAAG	189	59	Msc (F)	AGGAGGACCGCTACGAGG	156	66
lox (R)	CGTGTCTCCAGACAGAAGC			Msc (R)	CAATCCATCTAACTGCCCTGTC		
Gpr124 (F)	TCTGGTGAATGGGAGTGCTC	172	59	ligp1 (F)	CCTTCTCTGACCTTTCTCTTGG	132	59
Gpr124 (R)	AGGACTGGTAAGCCGTGATG			ligp1 (R)	ATCCACCTCTATTTCCCAGTCC		
Tpm2 (F)	AAAGTATTCCGAGTCCGTGA	180	59	Wnt2 (F)	ATCAAGTTTGCCCGTGCT	174	66
Tpm2 (R)	TTCTCAGCCTCCTCCAGC			Wnt2 (R)	CAGCCAGCATGTCTCAGAG		
RPL19 (F)	AAGCCTGTGACTGTCCATTC	146	59/66	Cdh1 (F)	GGCTTCAGTCCGAGGTCTACAC	154	66
RPL19 (R)	ATCCTCATCCTTCTCATCCAG			Cdh1 (R)	TGCCGTCTGTCGCCACTTT		

2.3 Protein Validation

After mRNA validation, the next phase was to check protein localization. The initial goal was to perform immunostaining for one gene from each primary and secondary compartment, but due to technical issues, western blotting was used for two genes to show protein localization.

2.3.1 Immunofluorescence (IF)

Optimal cutting temperature compound (OCT) embedded UGS samples were sectioned on a cryostat (CM3050 S, Leica Microsystems, Bannockburn, IL). Sections were made at 14 μ m and were stored at -80°C until use in IF to stain for specific protein localization. Immediately before staining, the sections were warmed to room temperature for five minutes and then fixed in pre-chilled methanol:acetone(1:1) solution for 20 minutes at -20°C. The sections were washed briefly in 1X phosphate buffered saline (PBS), pH 7.4, and blocked with 2-4% (v/v) serum from the same species as the secondary antibody (Jackson Immuno Research Laboratories, Inc., West Grove, PA) in PBS for one hour at room temperature. Primary antibody solutions, diluted in blocking buffer, were then added to cover the sections on the slides and were incubated for one hour at room temperature. Slides then underwent three, five minute washes (0.05% Tween-20 in PBS) followed by incubation with FITC or Texas Red donkey host secondary antibodies (1:200 dilution in blocking buffer) and incubated in dark for one hour at room temperature. Detailed information about the antibodies used in IF is listed in Table 2.2. The slides were then stained with TO-PRO3 (1:100,000) in PBS for ten minutes. Lastly, the slides underwent two final washes (0.05% Tween-20 in PBS) and were mounted with n-phenylenediamine mounting medium. A LSM 510

confocal microscope (Carl ZeissMicroimaging inc., Thornwood, NY) was used to image the slides.

For Tpm and Myh3, there was some difficulty in staining with mouse antibodies on mouse tissue. This issue was resolved by first blocking with 0.5% donkey anti mouse IgG. Furthermore, to allow co-staining with Cdh1, the procedure was the same as described above, except that after the secondary antibody incubation against the target protein there were three PBS washes and an incubation with FITC conjugated Cdh1, followed by the TO-PRO3 staining and mounting as described.

Table 2.2 Table showing antibody information. Information includes: antibody host, dilution (for Immunofluorescence), positive control tissue, supplier, and catalogue number. My standard procedure used a blocking solution of 5% normal donkey serum (Jackson) in 1x PBS with one hour blocking and incubations at room temperature. Variations include: Rabbit primary antibody (Pax2) also had 1% keratin in blocking buffer and antibody dilutions were left in primary incubation overnight; Mouse primary antibodies (Tpm, Myh, Cdh1) had 0.5% donkey anti-mouse IgG (Jackson) in the blocking buffer for the blocking step only. Supplier codes: [1] Abcam, [2] BD Biosciences, [3] Gregory R. Dressler, University of Michigan, Ann Arbor, MI, [4] Jackson ImmunoResearch.

Antibodies (Ab)	Origin	Dilution	+ Control Tissue	Supplier	Catalogue #
Primary Ab					
Tpm (1,2,3)	Mouse	1:100	embryonic muscle	1	ab7785
Myh3	Mouse	1:500	embryonic muscle	1	ab24642
Cdh1	Mouse	1:500	epethilium	2	610182
FITC conjugated Cdh1	Mouse	1:500	epethilium	2	612131
Pax2	Rabbit	1:2,000	kidney, brain	3	n/a
Secondary Ab					
Texas Red anti mouse	Donkey	1:200	n/a	4	715-075-151
FITC anti mouse	Donkey	1:200	n/a	4	715-095-150
FITC anti rabbit	Donkey	1:200	n/a	4	711-095-152

2.3.2 Western Blot (WB)

For the antibodies that did not work in IF, western blot (WB) was used to observe protein levels in different compartments. Protein was extracted from E16.5 UGS compartments in radioimmunoprecipitation (RIPA) buffer containing 50mM Tris HCl, pH 7.4, 150mM NaCl, 1mM EDTA, 1% Triton X-100, 1% sodium deoxycholate, 0.1% SDS, and 10% protease inhibitor cocktail (Roche, Indianapolis, IN). Protein concentration was determined using a BCA protein assay (Pierce, Rockford, IL). Samples were combined with loading buffer and reducing agent and then denatured at 95°C (Invitrogen). Proteins were resolved on 4-12% SDS-PAGE gradient gels (NuPAGE Bis-Tris Gel, Invitrogen). Protein was loaded at 20µg/well. Protein was transferred to nitrocellulose membrane (Whatman inc., Florham Park, NJ) using 30v for two hours. Membranes were blocked overnight at 4°C with PBS containing 5% nonfat dry milk (Nestle, Wilks-Barre, PA). Membranes were given 3 PBS-T (PBS + 0.1% Tween-20, Fisher) washes. Primary antibodies (from Table 2.2) were diluted in PBS (Myh3 at 1:1,000 and Pax2 at 1:2,000). The secondary antibody used was horseradish peroxidase (HRP-conjugated) either anti-goat for Pax2, or anti-mouse for Myh3, at 1:5,000 in PBS-T for one hour incubation. HRP was detected using ECL western blotting detection (Millipore, Piscataway, NJ) and exposure to film (Kodak, Rochester, NY).

Chapter 3

RESULTS

3.1 Custom cDNA Microarray (MA)

The microarray (MA) tested 10,290 unique mouse developmental genes and showed about 500 (4.8%) with UGE/UGM differences, and only 30 (0.29%) with UGD/UGV differences. We chose a threshold of three fold change difference for UGE/UGM and a threshold of two fold for UGD/UGV differences as significant, based on the observation that dorsal/ventral differences tended to be much smaller than epithelial/mesenchymal differences. With these thresholds, the MA results identified 173 UGE and 337 UGM candidates with >3 fold change, but only 25 UGD and 12 UGV candidates with >2 fold change. Some differentially expressed genes were grouped into functional categories by DAVID bioinformatics research (<http://david.abcc.ncifcrf.gov/>) and listed in Table 3.1. Twenty-two genes from the MA results were chosen for validation based on multiple factors: significant fold change difference, genes with known links to deregulation in cancer, available antibodies, and little previous knowledge on prostate localization.

Table 3.1 Selection of microarray results listed by functional categories. Table 3.1A shows a selection of the UGE/UGM microarray predictions. Table 3.1B shows the UGD/UGV microarray predictions. Results are statistically significant at FDR < 0.1%.

3.1A

UGM

UGE

	Symbol	Gene	Fold	Symbol	Gene	Fold
Growth Factor/	Bmp1	Bone morphogenetic protein 1	2.8	Cx3cl1	Chemokine (C-X3-C motif) ligand 1	4.0
Cytokine	Bmp4	Bone Morphogenetic protein 4	8.2	Igf2	Insulin-like growth factor 2	1.6
	Ccl2	Chemokine (C-C motif) ligand 2	2.9	Mif	Macrophage migration inhibitory factor	3.7
	Ctgf	Connective tissue growth factor	7.3	Pdgfa	Platelet derived growth factor, alpha	6.1
	Cxcl12	Chemokine (C-X-C motif) ligand 12	23.6	Shh	Sonic hedgehog	15.1
	Fst	Follistatin	2.1	Slurp1	Secreted Ly6/Plaur domain containing 1	3.2
	Gdf10	Growth differentiation factor 10	22.3	Wnt4	Wingless-related MMTV integration site 4	16.9
	Hgf	Hepatocyte growth factor	3.2			
	Igf1	Insulin-like growth factor 1	18.7			
	Igfbp3	Insulin-like growth factor binding protein 3	28.4			
	Igfbp6	Insulin-like growth factor binding protein 6	3.2			
	Il16	Interleukin 16	3.3			
	Pdgfd	Platelet-derived growth factor, D polypeptide	2.8			
	Penk1	Preproenkephalin 1 (Opioid growth factor)	9.3			
	Sfrp1	Secreted frizzled-related sequence protein 1	1.7			
	Sfrp2	Secreted frizzled-related sequence protein 2	2.3			
	Tgfb2	Transforming growth factor, beta 2	2.9			
	Wnt2	Wingless-related MMTV integration site 2	4.3			

3.1A (continued)

	Symbol	Gene	Fold UGE	Symbol	Gene	Fold UGM	
Growth Factor Receptor	Acvr1	Activin A receptor, type II-like 1	7.7	Acvr2b	Activin receptor IIB	2.8	
	Agtr2	Angiotensin II receptor, type 2	15.9	Adra2a	Adrenergic receptor, alpha 2a	4.4	
	Fgfr1	Fibroblast growth factor receptor 1	3.3	Fgfr2	Fibroblast growth factor receptor 2	1.9	
	Il11ra1	Interleukin 11 receptor, alpha chain 1	7.5	Sdfr2	Stromal cell derived factor receptor 2	6.1	
	Pdgfrb	Platelet derived growth factor receptor, beta	16.3				
	Ptch1	Patched homolog 1	2.2				
	Tgfr2	Transforming growth factor, beta receptor II	4.4				
Transcription Factor	Cdx2	Caudal type homeo box 2	11.8	Fos	FBJ osteosarcoma related oncogene	3.2	
	Fhl2	Four and a half LIM domains 2	11.4	Foxa1	Forkhead box A1	35.2	
	Foxd1	Forkhead box D1	5.1	Gata3	GATA binding protein 3	3.3	
	Foxd2	Forkhead box D2	12.5	Irf6	Interferon regulatory factor 6	23.9	
	Hand2	Heart and neural crest derivatives expressed 2	10.3	Irx2	Iroquois related homeobox 2 (Drosophila)	24.2	
	Lef1	Lymphoid enhancer binding factor 1	6.7	Junb	Jun-B oncogene	4.5	
	Myod1	Myogenic differentiation 1	4.8	Sox9	SRY-box containing gene 9	4.4	
	Nr2f1	Coup-TF2, group F, member 1	7.2	Tcfap2c	Transcription factor AP-2, gamma	6.3	
	Phox2b	Paired-like homeobox 2b	12.0	Tcfcp2l3	Transcription factor CP2-like 3	29.3	
	Tbx2	T-box 2	4.4	Zfp67	Zinc finger protein 67	6.2	
	Zfx1a	Zinc finger homeobox 1a	12.3				
	Cytoskeletal	Acta2	Actin, alpha 2, smooth muscle, aorta	23.0	Capg	Capping protein (actin filament), gelsolin-like	5.0
		Aif1	Allograft inflammatory factor 1	6.0	Dnahc11	Dynein, axonemal, heavy chain 11	3.3
Des		Desmin	3.3	Evpl	Envoplakin	15.0	
Kif5c		Kinesin family member 5C	6.5	Myh14	Myosin, heavy polypeptide 14	9.8	
Myh11		Myosin heavy chain 11, smooth muscle	30.5	Spr2a	Small proline-rich protein 2B	9.4	
My14		Myosin, light polypeptide 4	6.2				

3.1A (continued)

	Symbol	Gene	Fold UGE	Symbol	Gene	Fold UGM
Cytoskeletal (continued)	Mylk	Myosin, light polypeptide kinase	12.9			
	Nefl	Neurofilament, light polypeptide	32.3			
	Plekhc1	Pleckstrin homology domain containing, family C (with FERM domain) member 1	6.1			
	Tagln	Transgelin	42.4			
	Tnnc1	Troponin C, cardiac/slow skeletal	7.1			
	Tnnc2	Troponin C2, fast	22.8			
	Tnnt2	Troponin T2, cardiac	18.1			
	Tpm2	Tropomyosin 2, beta	23.9			
Extracellular Matrix Related/ Cell Adhesion	Adamts8	A disintegrin-like and metalloprotease (reprolysin type) with thrombospondin type 1 motif, 8	10.0	Alcam	Activated leukocyte cell adhesion molecule	2.8
				Cdh1	Cadherin 1 (E-cadherin)	7.3
				Cdh3	Cadherin 3 (P-cadherin)	3.8
	Aplp1	Amyloid beta (A4) precursor-like protein 1	5.3	Col18a1	Procollagen, type XVIII, alpha 1	3.2
	Cdh2	Cadherin 2 (N-cadherin)	7.2	Col4a5	Procollagen, type IV, alpha 5	3.8
	Cdh5	Cadherin 5 (VE-cadherin)	5.8	Itga3	Integrin alpha 3	4.6
	Col11a1	Procollagen, type XI, alpha 1	3.2	Itga6	Integrin alpha 6	3.2
	Col1a1	Procollagen, type I, alpha 1	7.6	Itgb4	Integrin beta 4	13.7
	Col1a2	Procollagen, type I, alpha 2	54.4	Lu	Lutheran blood group (Auburger b included)	5.1
	Col23a1	Procollagen, type XXIII, alpha 1	10.7	Mmp7	Matrix metalloproteinase 7	2.9
	Col3a1	Procollagen, type III, alpha 1	63.1			
	Col4a1	Procollagen, type IV, alpha 1	3.1			
	Col4a2	Procollagen, type IV, alpha 2	2.6			
	Col5a1	Procollagen, type V, alpha 1	5.3			
	Col6a1	Procollagen, type VI, alpha 1	26.7			
	Col6a3	Procollagen, type VI, alpha 3	21.7			
	Col8a2	Procollagen, type VIII, alpha 2	3.4			
	Cspg4	Chondroitin sulfate proteoglycan 4	4.2			

3.1A (continued)

	Symbol	Gene	Fold UGM	Symbol	Gene	Fold UGE
Extracellular	Dcn	Decorin	3.5			
Matrix Related/	Eln	Elastin	10.3			
Cell Adhesion	Emilin2	Elastin microfibril interfacier 2	7.2			
(continued)	Fbln2	Fibulin 2	4.1			
	Fstl1	Follistatin-like 1	4.0			
	Itga8	Integrin alpha 8	3.7			
	Itga9	Integrin alpha 9	6.7			
	Jam3	Junction adhesion molecule 3	11.1			
	Lamc3	Laminin gamma 3	3.6			
	Lox	Lysyl oxidase	66.3			
	Mfap4	Microfibrillar-associated protein 4	36.7			
	Mfap5	Microfibrillar associated protein 5	4.9			
	Mmp16	Matrix metalloproteinase 16	6.5			
	Mmp2	Matrix metalloproteinase 2	13.7			
	Mmp23	Matrix metalloproteinase 23	2.7			
	Nid1	Nidogen 1	6.8			
	Nkd1	Naked cuticle 1 homolog (Drosophila)	6.2			
	Postn	Periostin, osteoblast specific factor	12.9			
	Prg1	Proteoglycan 1, secretory granule	4.7			
	Sparc11	SPARC-like 1 (mast9, hevin)	59.5			
	Tgfb1	Transforming growth factor, beta induced	27.7			
	Timp2	Tissue inhibitor of metalloproteinase 2	3.0			
	Timp3	Tissue inhibitor of metalloproteinase 3	4.0			

3.1B

UGD

UGV

22

	Symbol	Gene	Fold	Symbol	Gene	Fold
Cell Adhesion/	Clu	Clusterin	2.0	Aldh1a1	Aldehyde dehydrogenase family 1, subfamily a1	2.3
Cytoskeletal	Igfbp3	Insulin-like growth factor binding protein 3	2.1	Myh3	Myosin, heavy polypeptide 3, skeletal muscle, embryonic	2.2
	Itga8	Expressed sequence ai447669	2.2			
	Spp1	Secreted phosphoprotein 1	3.1	Mylpf	Myosin light chain, phosphorylatable, fast skeletal muscle	2.0
	Tgfb1	Transforming growth factor, beta induced	2.2			
	Thy1	Thymus cell antigen 1, theta	2.4	Tnnc1	Troponin c, cardiac/slow skeletal	2.0
	Tinag	Tubulointerstitial nephritis antigen	2.5	Tnnc2	Troponin c2, fast	2.2
				Wnt4	Wingless-related mmtv integration site 4	1.5
Transcription	Dlx5	Distal-less homeobox 5	3.2	Esr1	Estrogen receptor 1 (alpha)	2.1
Factor	Hand2	Heart and neural crest derivatives expressed transcript 2	2.0	Irx2	Iroquois related homeobox 2 (drosophila)	2.1
	Lef1	Lymphoid enhancer binding factor 1	2.0	Msc	Musculin	1.8
	Nr2f1	Nuclear receptor subfamily 2, group f, member 1	2.1	Mt1	Metallothionein 1	2.1
				Mt2	Metallothionein 2	2.1
Lipid Binding	Crabp1	Cellular retinoic acid binding protein i	2.6			
	Ly6e	Lymphocyte antigen 6 complex, locus e	1.6			
	Pnlip	Pancreatic lipase	2.2			
Intercellular	C1qtnf3	C1q and tumor necrosis factor related protein 3	2.3			
	Nkd1	Naked cuticle 1 homolog (Drosophila)	1.6			
	Ntrk2	Neurotrophic tyrosine kinase, receptor, type 2	2.9			
	Plac8	Placenta-specific 8	3.4			
	Sbp	Spermine binding protein	2.4			
	St6gal1	Beta galactoside alpha 2,6 sialyltransferase 1	1.7			
	Tulp2	Tubby-like protein 2	2.1			

3.2 Quantitative PCR (Q-PCR)

The goal of this project was to validate the MA results, and the first step was to select a few genes and check mRNA levels by Q-PCR to demonstrate a proof of principal for the MA. Of the genes tested in Q-PCR for UGE/UGM differences, 6 of 6 matched the subdomains as predicted by the microarray results (Fig. 3.1A). All six genes showed fold changes of >6 fold. The actual fold change varied from the MA prediction (Table 3.1), but all the genes were found in the predicted tissue compartments. Of the genes tested for D/V difference, 5 of 6 were found in the predicted region (Fig. 3.1B), though only one showed >4 fold difference (Pax2). Furthermore, the one that did not match the prediction (Tnfrsf19) only showed a 1.2 fold difference, which along with the observed error in range of expression seems unlikely to be significant D/V difference.

For the secondary compartment predicted genes, Fgfr2 (predicted DE) showed clear UGE, but little D/V difference; meanwhile Krtdap (predicted DE) showed dorsal restricted expression but barely UGE (Fig. 3.2A). For the VE genes, Wnt4 matched both predictions, while Tacstd1 was indeed UGE, but surprisingly showed about 4 fold dorsal specific expression (Fig. 3.2B). All 4 of 4 DM predicted genes matched in both categories (Fig. 3.3A). For the VM genes, all 3 showed UGM localization, but only Iigp1 showed clear ventral localization, while the other 2 showed no clear D/V difference (Fig. 3.3B). Results were also depicted in a Cartesian quadrant format (Fig. 3.4) to give a better visualization of how well each fit into the predicted compartment.

3.2.1 Male Female Differences

As I will explain later in the discussion, some of the discrepancies between the MA predictions and the Q-PCR results were likely due to male UGS template being used in the Q-PCR experiments, but combined male/female template being used for the MA. Fig. 3.5A depicts two genes that showed mRNA localization in opposite UGE/UGM compartments in male versus female template. Pax2 showed about 32 fold UGE in male tissue, but about 39 fold UGM in female. Furthermore, Myh3 showed slightly (~3 fold) UGE in females, but about 256 fold UGM in male UGS. Fig. 3.5B shows three genes with male/female differences in UGD/UGV localization. Tacstd1 shows about 4 fold UGD in male, but about 48 fold UGV in female. Pax2 appeared UGD localized in both male and female, but only about 8 fold in female as opposed to a much higher 256 fold UGD localization in males. Lastly, Fgfr2 showed no UGD/UGV difference in males, but it was 8 fold UGD in females.

3.2.2 Cross Check for Primary Compartment Genes

After the Myh3 IF results were observed, where Myh3 showed an unexpected UGM localization in addition to the predicted UGV localization, we suspected some genes might also show differential expression in the other compartments despite the MA predictions. Thus, we cross checked the primary genes in the unpredicted compartments as well (Fig. 3.6). Of the originally pure UGD/UGV predicted genes, 3 showed >3 fold change difference in UGE/UGM as well (Myh3 at 222 fold UGM, Tnnc2 at 17 fold UGM, and Tnsrf19 at 3 fold UGE). Of the 6 UGE/UGM genes, none showed >3 fold difference in UGD/UGV. Gpr124 showed the most differential expression with 2.8 fold UGD. All the data points had large error bars thus appearing to show little or no true UGD/UGV difference.

Table 3.2 – Reference table for Log_2 scale => fold change conversion. The results in the Q-PCR figures (3.1-3.6) are recorded as $\Delta\Delta$ cycle threshold (CT) values, which equal a Log_2 exponential scale for fold change. This table serves as a quick reference to compare $\Delta\Delta\text{CT}$ values with fold changes (FC). $\text{FC} = \text{Log}_2(\Delta\Delta\text{CT})$.

<u>$\Delta\Delta\text{CT}$</u>	<u>FC</u>
1	2
<i>1.5</i>	<i>2.8</i>
2	4
<i>2.5</i>	<i>5.7</i>
3	8
<i>3.5</i>	<i>11.3</i>
4	16
<i>4.5</i>	<i>22.6</i>
5	32
<i>5.5</i>	<i>45.3</i>
6	64
<i>6.5</i>	<i>90.5</i>
7	128
<i>7.5</i>	<i>181</i>
8	256
<i>8.5</i>	<i>362</i>
9	512
<i>9.5</i>	<i>724</i>
10	1024

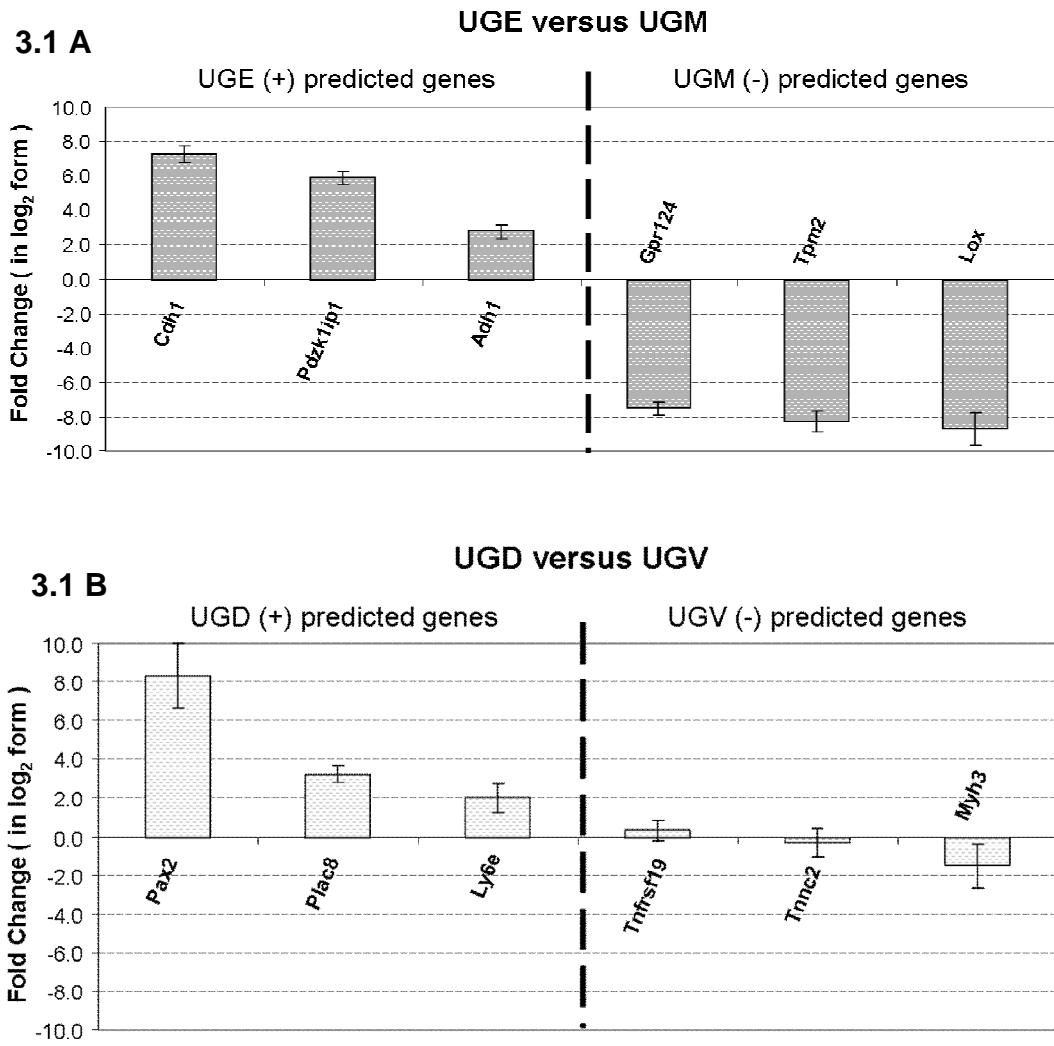


Fig. 3.1 Primary Compartment mRNA localization by Q-PCR. Primers from table 2.1 were used in Real-Time Quantitative PCR (Q-PCR) with primary compartment genes. Graph 3.1A shows the pure predicted UGE/UGM genes, while 3.1B shows the pure predicted UGD/UGV genes. Results were normalized to RPL19. Y-axis shows fold change in log₂ form (e.g. 3 = 2³, or 8 fold difference). Error bars show standard error from one run of Q-PCR in duplicate per gene with male E16.5 template.

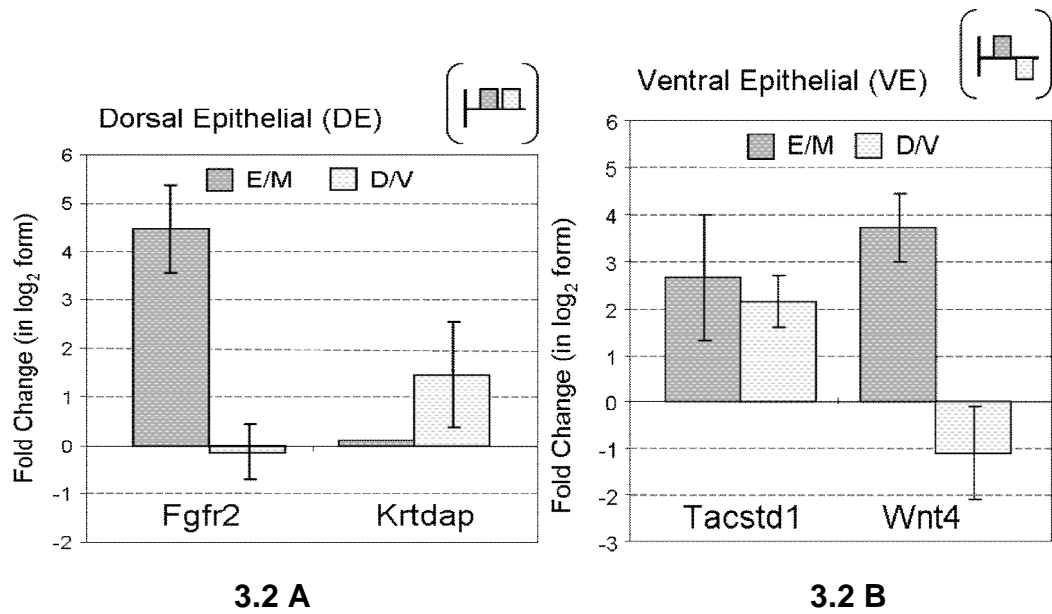


Fig. 3.2 Epithelial secondary compartment mRNA localization by Q-PCR. Primers from table 2.1 were used in Real-Time Quantitative PCR (Q-PCR) with epithelial predicted secondary compartmental genes (DE, VE). Gray bars are E/M fold differences (+/-), and white bars are D/V difference (+/-). Results were normalized to RPL19. Y-axis shows fold change in \log_2 form (e.g. $3 = 2^3$, or 8 fold difference). Error bars show standard error from one run of Q-PCR in duplicate per gene with male E16.5 template, with the exception of Krtdap for E/M, which was a single run (no error bars).

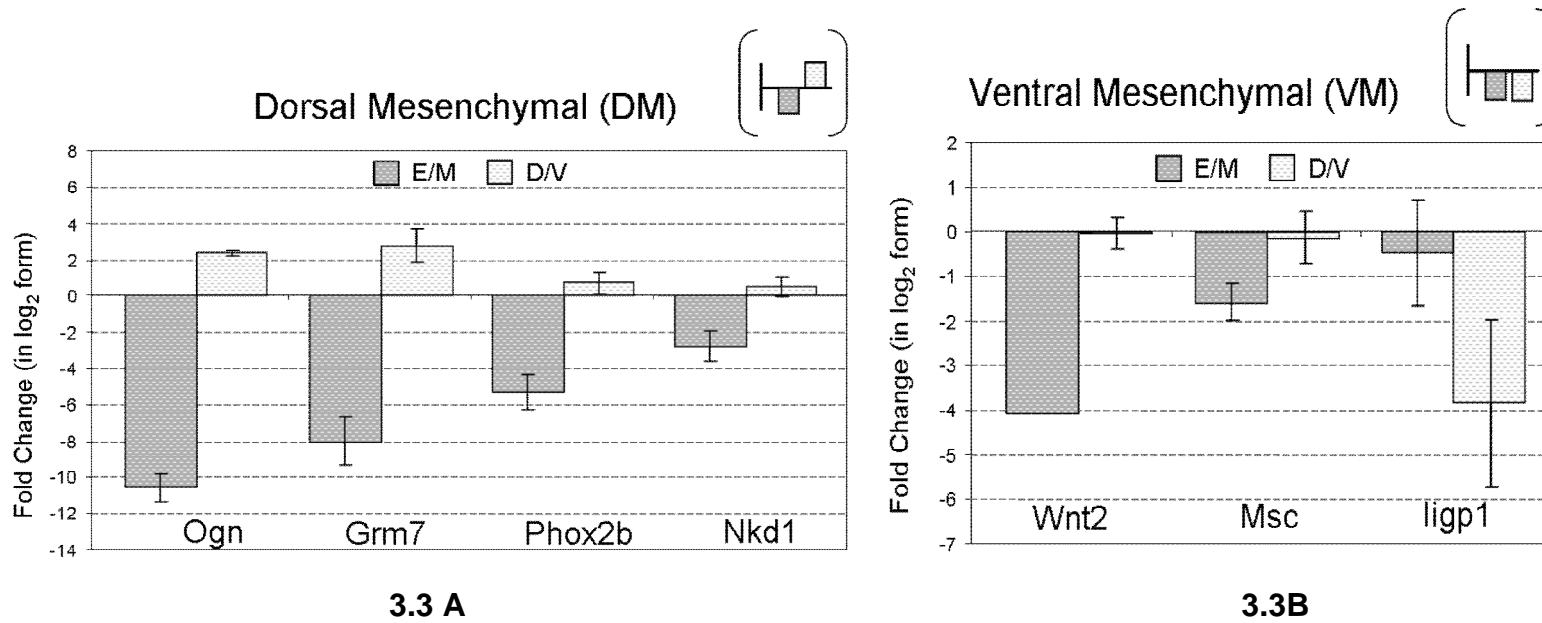


Fig. 3.3 Mesenchymal secondary compartment mRNA localization by Q-PCR. Primers from table 2.1 were used in Real-Time Quantitative PCR (Q-PCR) with mesenchymal predicted secondary compartment genes (DM, VM). Gray bars are E/M fold differences (+/-), and white bars are D/V difference (+/-). Results were normalized to RPL19. Y-axis shows fold change in log₂ form (e.g. 3 = 2³, or 8 fold difference). Error bars show standard error from one run of Q-PCR in duplicate per gene with male E16.5 template, with the exception of Wnt2 for E/M, which was a single run (no error bars).

Q-PCR Secondary Compartment Results in a Cartesian Quadrant Graph

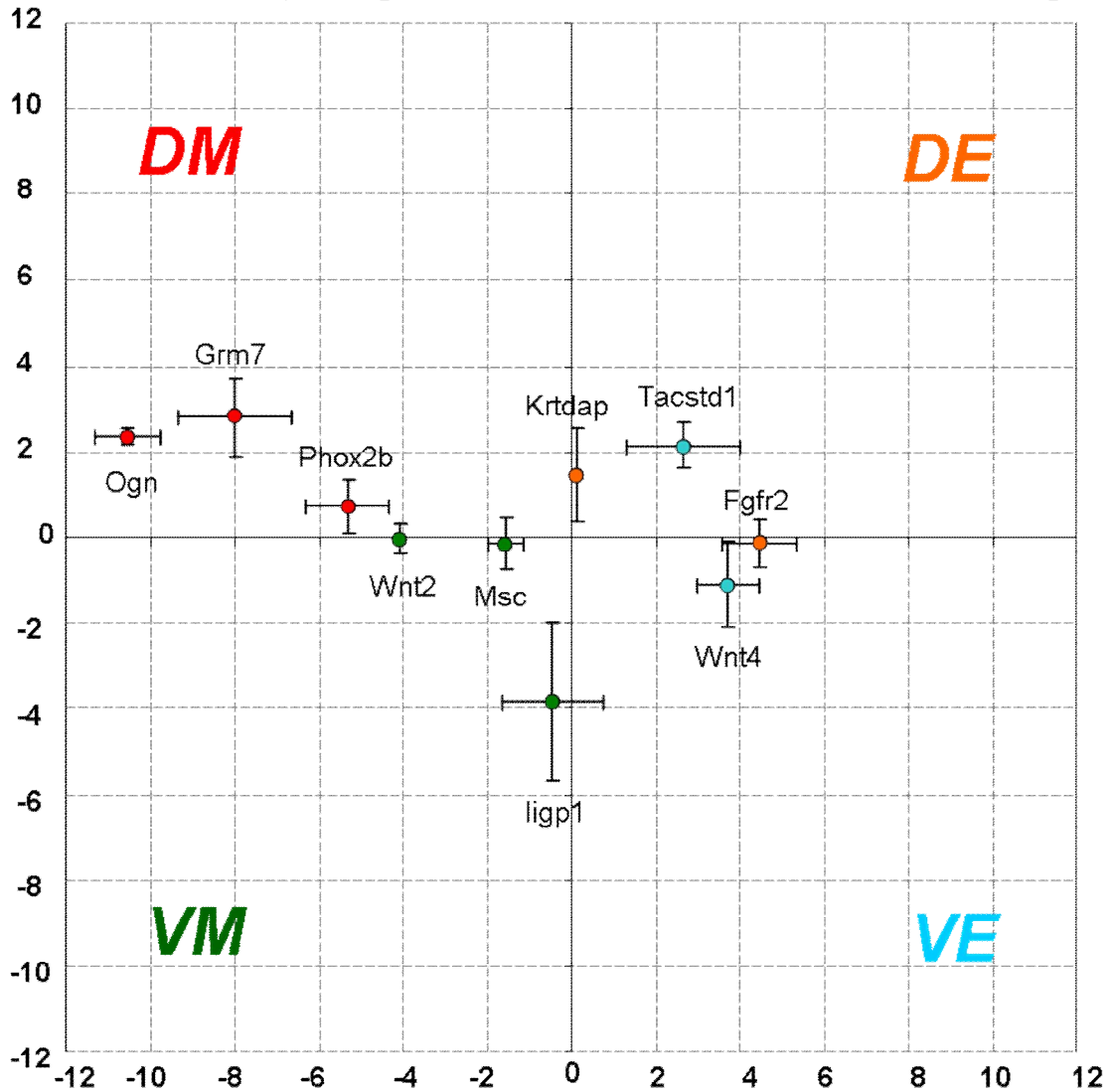


Fig. 3.4 Q-PCR results for secondary compartment genes in Cartesian. Both axes are in \log_2 fold change form. X-axis shows E/M differences, with + axis for UGE, - axis for UGM. Y-axis shows D/V differences, with + axis for UGD, - axis for UGV. Values and error bars are same as in Figs. 3.2 and 3.3. Predicted compartments: DE =orange, DM=red, VM=green, VE=blue

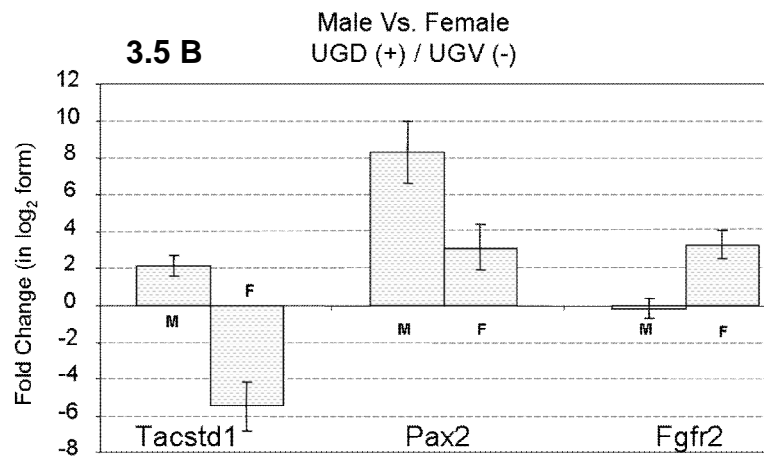
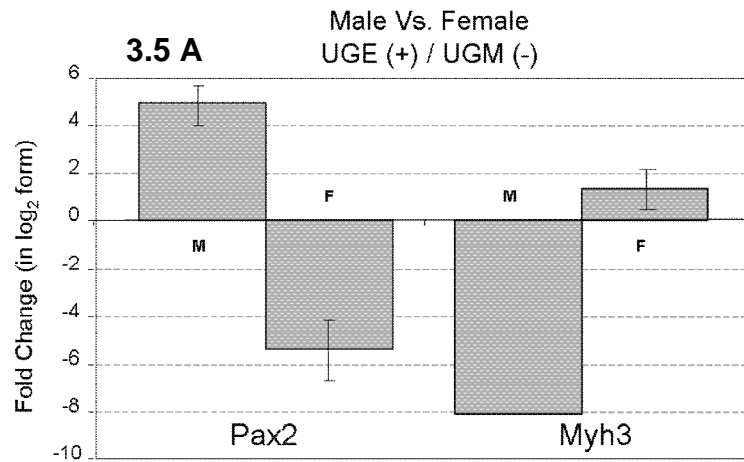


Fig. 3.5 Q-PCR results of male versus female mRNA differences. Fig. 3.5A depicts UGE/UGM (+/-) differences for Pax2 and Myh3 in male versus female template. Fig. 3.5B depicts sex differences in UGD/UGV (+/-) for Tacstd1, Pax2, and Fgfr2. M=male, F=female. Results were normalized to RPL19. Y-axis shows fold change in log₂ form (e.g. 3 = 2³, or 8 fold difference). Error bars show standard error from one run of Q-PCR with E16.5 template and each gene run in duplicate, with the exception of Myh3 Male, which was a single run (no error bars).

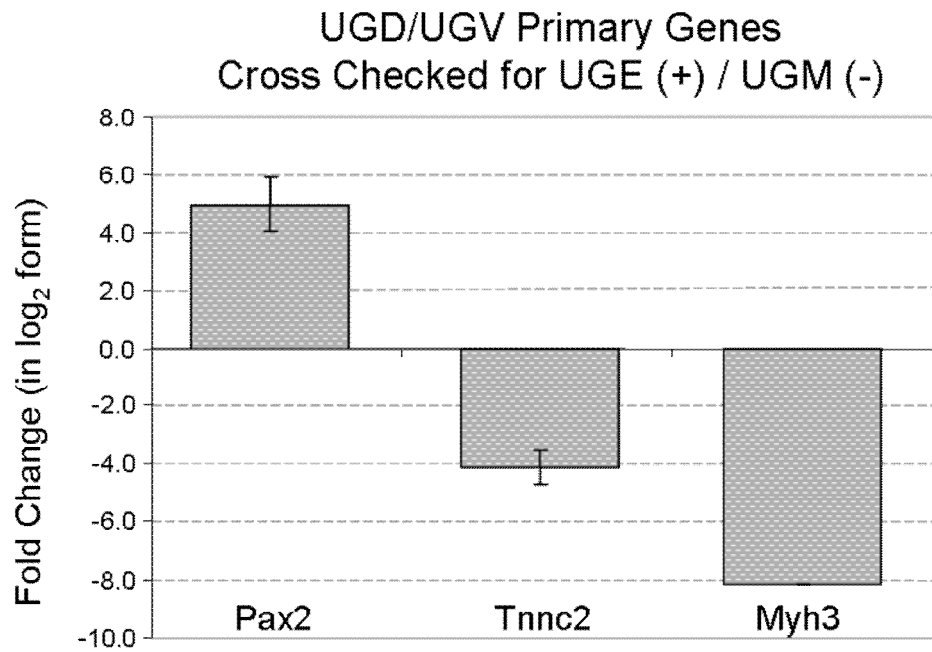


Fig. 3.6 Q-PCR results of UGD/UGV primary genes cross checked for UGE/UGM differences. The figure depicts the 3 UGD/UGV genes (Pax2, Tnnc2, Myh3) that showed >4 fold UGE/UGM (+/-) differences, despite being predicted purely UGD/UGV by the microarray. Results were normalized to RPL19. Y-axis shows fold change in log₂ form (e.g. 3 = 2³, or 8 fold difference). Error bars show standard error from one run of Q-PCR with E16.5 male template and each gene run in duplicate, with the exception of Myh3, which was a single run (no error bars).

3.3 Immunofluorescence (IF)

Immunofluorescence initially was attempted for validation of one gene for each compartment: Cdh1 (UGE), Tpm (UGM), Pax2 (UGD), Myh3 (UGV), Fgfr2 (DE), Wnt4 (VE), Msc (VM), Ntrk2 (DM). Selection was based on fold change as well as antibody availability. Due to antibody difficulties in IF, Pax2 and Myh3 were confirmed by western blot, while Wnt4 and Ntrk2, despite working on positive control tissue, failed to work in any immunostaining. Cdh1 is a known epithelial gene and showed clear UGE staining (Figure 3.7 all), so it was then used as an epithelial marker for the other genes (32). The Tpm antibody recognized Tpm1 and Tpm2 isoforms, and it showed clear mesenchymal staining (Fig. 3.7A). Myh3 showed unpredicted strong UGM localization and no significant UGV/UGD difference despite being predicted UGV by mRNA results (Fig. 3.7B). Msc showed nice staining in a band in the VM region of the UGS (Fig. 3.7C). Fgfr2 showed interesting staining in a long cut of E18.5 UGS, with staining on the UGE/UGM border and at dorsal budding (Fig. 3.7D).

Figure 3.7A – Tpm2 (UGM) and Cdh1 (UGE) staining

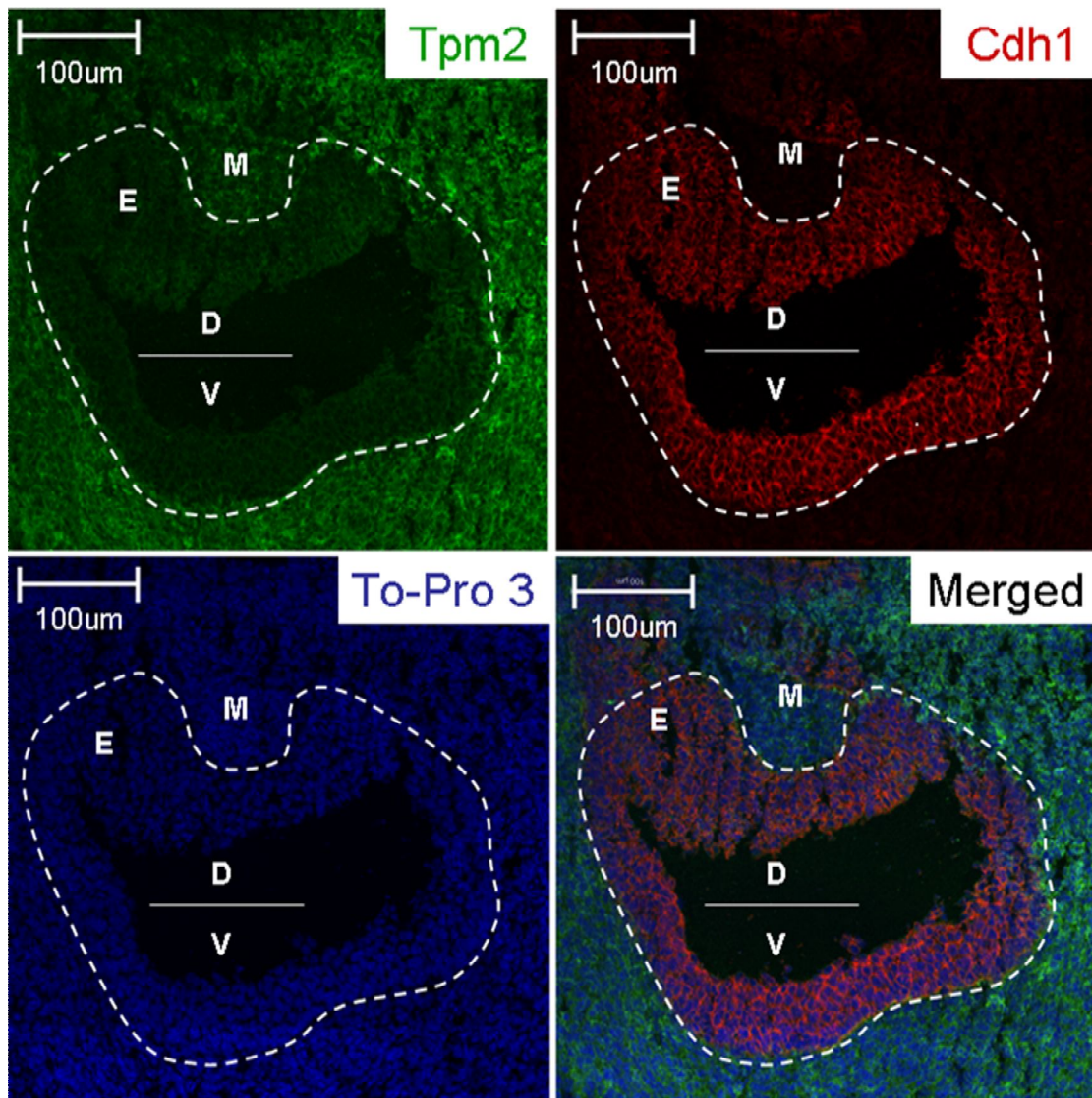


Fig. 3.7A IF staining for Tpm2 (UGM predicted) and Cdh1 (UGE predicted). Blue staining shows nuclear staining with To-Pro 3. Tissue is a cross section of E16.5 male UGS tissue. E = UGE, M = UGM, D =dorsal, V = ventral.